1.5 J high-beam-quality Nd:LuAG ceramic active mirror laser amplifier

Jianlei Wang (王建磊)[1,2,*], Kaiqi Zhao (赵开祺)[2,3], Tao Feng (冯涛)[2,4], Xiaolei Zhu (朱小磊)[1,2], and Weibiao Chen (陈卫标)[1,2]

[1]*Key Laboratory of Space Laser Communication and Detection Technology, Chinese Academy of Sciences, Shanghai 201800, China*

[2]*Shanghai Institute of Optics and Fine Mechanics, Chinese Academy of Sciences, Shanghai 201800, China*

[3]*Shanghai Key Laboratory of All Solid-State Laser and Applied Techniques, Shanghai 201800, China*

[4]*Key Laboratory of Materials for High Power Laser, Chinese Academy of Sciences, Shanghai 201800, China*

**Corresponding author: wangjl@siom.ac.cn*

Received August 28, 2019; accepted November 1, 2019; posted online December 24, 2019

A 1.5 J Nd:LuAG ceramic active mirror laser amplifier with a high beam quality is demonstrated in which a 0.8% (atomic fraction) Nd-doped Nd:LuAG ceramic disk with a diameter of 64 mm and a thickness of 5.5 mm is used as a laser gain medium. A maximum single-pass small-signal gain of 2.59 is measured when the pump energy is 11.5 J, with an injected seed energy of 0.4 J; a maximum output energy of 1.5 J is obtained at the repetition rate of 10 Hz. A far-field beam spot 1.25 times the diffraction limit (DL) is achieved by using a stimulated Brillouin scattering phase conjugation mirror (SBS-PCM) for wavefront correction.

Keywords: high energy lasers; disk laser amplifiers; Nd:LuAG ceramic; high beam quality.
doi: 10.3788/COL202018.021401.

High-energy repetitive nanosecond pulse lasers with a good beam quality are required for many applications[1–9] including free space communications, space debris detection, particle acceleration, material processing, Thomson scattering diagnostic systems, etc. Master oscillator power amplifier (MOPA)[10] configuration lasers are so far the most promising way to scale laser energy while maintaining a good beam quality.

In order to achieve high energy at the repetition rate, the choice of amplifier gain medium and its geometry are important. Until now, several solid-state laser materials[10,11] have been widely used, such as Nd:YAG, Yb:YAG, Nd:YVO4, and Nd:YLF, among which Nd:LuAG is considered to be a potential material for high-energy repetitive lasers[11,12], due to its advantages of a moderate emission cross section, a relatively long fluorescence lifetime of 277 μs, as well as outstanding physical and chemical properties.

Lasers using a Nd:LuAG crystal as the gain medium have been increasingly investigated recently. Typically, Q-switched Nd:LuAG lasers with a maximum output energy of 70 mJ at a 50 Hz repetition rate[13] and an output pulse energy of 13 mJ at a 500 Hz repetition rate[14] were, respectively, reported. In 2016, a diode-pumped laser[15] based on Nd:YAG–Nd:LuAG crystal hybrid active mirror amplifiers obtained an output energy of more than 1.5 J at the repetition rate of 10 Hz.

In this Letter, a Nd:LuAG ceramic active mirror disk laser amplifier in a MOPA configuration is investigated. In order to obtain a high-energy laser output while maintaining a good beam quality, image relaying systems and stimulated Brillouin scattering phase conjugation mirrors (SBS-PCMs)[16] are used for wavefront correction. A maximum output energy of 1.5 J in a 10 ns pulse duration is obtained at the repetition rate of 10 Hz when the pump energy is 11.5 J, where a maximum pulse energy more than 1 J has been extracted in the Nd:LuAG amplifier, and a far-field beam spot 1.25 times the diffraction limit (DL) has been achieved.

The schematic diagram of the laser is shown in Fig. 1, which is based on the MOPA configuration and consists of a conductively cooled single-frequency main oscillator, a preamplifier, a beam control unit, and the Nd:LuAG ceramic disk amplifier. The oscillator and preamplifier uses a conductively cooled, diode pumped Nd:YAG slab laser[5]. A single longitudinal-mode laser of 10 mJ in a 12 ns duration is generated from the oscillator and is amplified to 450 mJ by the following three zigzag slab pre-amplifiers.

After passing through two Faraday isolators, the output laser beam is shaped by a serrated aperture and

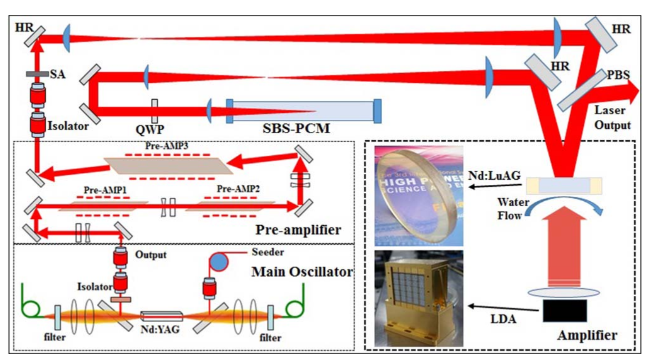

Fig. 1. Schematic diagram of the laser. HR: high reflector, PBS: polarized beam splitter, QWP: quarter-wave plate, LDA: laser diode array, SA: serrated aperture.

the pulse energy is reduced to 400 mJ. The beam at the serrated aperture is then relay-imaged to the amplifier surface and the beam is expanded from 7 mm to 31 mm with an imaging system. After the first pass of the gain medium, the laser beam is reduced 2 times by the other image-relay system. The relay-imaged laser beam is focused by a focusing lens of 500 mm into an SBS cell filled with Fluorinert liquid (FC-770, 3M Electronics), where a phase conjugate return is generated and reflected. The polarization of the reflected beam is changed from horizontal to vertical by a quarter-wave plate, while after the second pass amplification the beam exits the amplifier through a polarized beam splitter (PBS).

A Nd:LuAG ceramic disk with a diameter of 64 mm and a thickness of 5.5 mm serves as the amplifier gain, which consists of a 50 mm diameter Nd-doped inner region that is surrounded by a 7 mm wide Sm-doped cladding to minimize amplified spontaneous emission (ASE) loss and prevent parasitic oscillations at high gain. The Nd: LuAG ceramic disk is fabricated by the solid-state sintering method. The powder is first vacuum sintered at 1750°C for 5 h under a vacuum of 10^{-3} Pa. Then it is hot isostatic pressing (HIP) sintered at 1750°C under 200 MPa in an argon atmosphere for 2 h as an after-treatment method. The fabricated ceramic sample is finally mirror-polished on both surfaces, and the in-line transmittance curve and microstructure are shown in Fig. 2, where the transmittance at a wavelength of 1064 nm is 81.6%, leading to a loss factor of 0.0485 cm^{-1}.

The front surface of the ceramic gain that the laser enters at a 15° incidence angle is antireflection (AR)-coated for 1064 nm and high reflection (HR)-coated for 808 nm relative to air, while the back surface is HR-coated for 1064 nm and AR-coated for 808 nm relative to water, where an 808 nm laser diode array is used to pump the gain from the back surface, producing a 32 mm × 35 mm square. For efficient thermal management, the gain is cooled by forced flowing water between the gain and a quartz window that directly flows over the disk back surface at a typical volume flow rate of 10 L/min and a pressure of 0.15 MPa.

The transmission of the amplifier after two passes is measured as 89%, corresponding to a loss factor of 0.05 cm^{-1}, which implies the passive losses of the amplifier

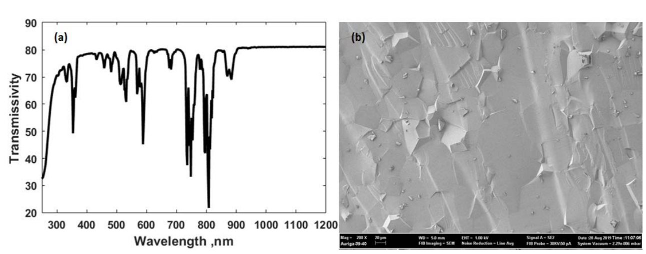

Fig. 2. (a) Transmittance curve and (b) microstructure of Nd: LuAG ceramic.

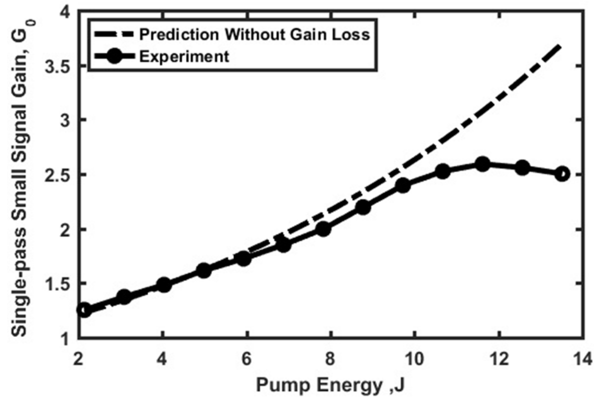

Fig. 3. Small signal gain versus pump energy.

such as bulk optical scattering losses, the interface losses of the optics, and the depolarization losses.

To evaluate the stored energy in the gain, the single-pass small signal gain G_0 is tested, which is defined as[10]

$$G_0 = E_{\mathrm{out}}/E_{\mathrm{in}} = \exp(g_0 l), \quad (1)$$

where E_{in} is the low-input signal, E_{out} is the amplified output laser, g_0 is the small-signal gain coefficient, and l is the single-pass gain length through the gain. Here, $l = 2t/\cos\theta$ for active mirror laser gain, t is the thickness of the gain, and θ is the laser incidence angle in the gain.

Figure 3 shows G_0 with different pump energies. The input laser energy is 4 mJ. G_0 increases greatly as the pump energy increases when the pump energy is less than 8 J, and the gain saturation is observed when the pump energy is greater than 11.5 J, where $G_0 = 2.59$ is obtained.

For nanosecond-pulse amplification studies, the amplifier is seeded by the pulsed output from the preamplifier, as is shown in Fig. 4, where the pump energy is 11.5 J. A linear amplification of output energy is observed for the first pass of the amplifier. When the input energy is 0.4 J, the output energy of the single pass is 0.8 J. After the second pass of amplification, an output energy of 1.5 J is achieved with an extraction energy of 1.1 J, corresponding to an optical to optical efficiency of 9.5%, due to the

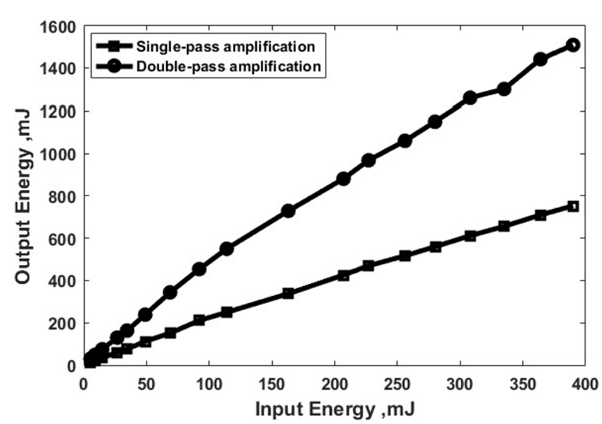

Fig. 4. Output performance versus input energy.

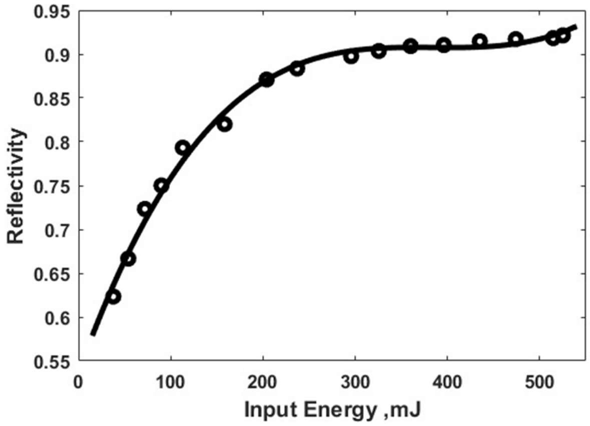

Fig. 5. Reflectivity of the SBS-PCM as a function of input energy.

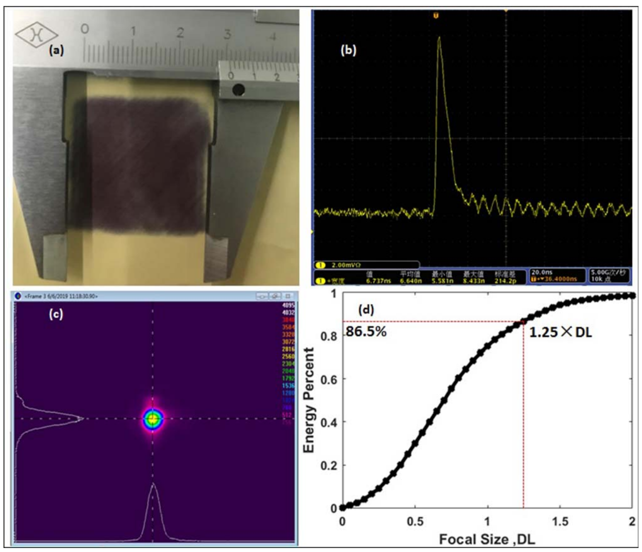

Fig. 6. (a) NFP, (b) compressed pulse duration, (c) FFP, and (d) encircled focal spot energy fraction of the double-pass amplified laser pulse with SBS-PCM.

bulk optical scattering losses from which the scattered laser light will be amplified and lead to severe losses of the stored energy.

The one-pass amplified output laser is focused at a point 450 mm inside the 800 mm long SBS-PCM cell where a phase conjugate return is generated. Figure 5 shows the measured reflectivity of the SBS-PCM as a function of input energy for 14 ns pulses, the SBS threshold energy is approximately 15 mJ, and a maximum reflectivity of 92% is observed at an input pulse energy of 500 mJ at 10 Hz repetition rate.

The near-field pattern (NFP), far-field pattern (FFP), and pulse duration of the double-pass amplified laser pulse with SBS-PCM are shown in Fig. 6. The focal size of the 86.5% encircled energies is 1.25 times the value of the diffraction limit when the output energy is 1.5 J, while the pulse duration is compressed to 6.64 ns.

In summary, we have demonstrated a joule-level Nd:LuAG ceramic active mirror laser amplifier with high beam quality. When the pump energy is 11.5 J, the 1.5 J energy and 6.64 ns pulse at a 10 Hz repetition rate is obtained in double-pass amplification, and the far-field beam spot 1.25 times the DL has been achieved by taking advantage of the SBS-PCM to compensate the laser beam distortion. Our next work will pay more attention to reducing optical scattering losses of the Nd:LuAG ceramic, which will lead to a higher laser output performance.

References

1. S. Banerjee, P. D. Mason, K. Ertel, P. Jonathan Phillips, M. De Vido, O. Chekhlov, M. Divoky, J. Pilar, J. Smith, T. Butcher, A. Lintern, S. Tomlinson, W. Shaikh, C. Hooker, A. Lucianetti, C. Hernandez-Gomez, T. Mocek, C. Edwards, and J. L. Collier, Opt. Lett. **41**, 2089 (2016).
2. A. Bayramian, R. Bopp, M. Borden, B. Deri, R. DesJardin, J. M. Di Nicola, M. Drouin, A. Erlandson, S. Fulkerson, J. Jarboe, G. Johnson, H. Zhang, B. Heidl, J. Horner, K. Kasl, D. Kim, E. Koh, J. Lusk, C. Marshall, D. Mason, T. Mazanec, J. Naylon, J. Nissen, K. Primdahl, B. Rus, M. Scanlan, K. Schaffers, T. Simon, T. Spinka, J. Stanley, C. Stolz, S. Telford, and C. Haefner, in *Conference on Lasers and Electro-Optics* (2016), paper STu3M.2.
3. X. Cheng, J. Wang, Z. Yang, J. Liu, L. Li, X. Shi, W. Huang, J. Wang, and W. Chen, High Power Laser Sci. Eng. **2**, e18 (2014).
4. X. Ma, J. Wang, J. Zhou, X. Zhu, and W. Chen, Appl. Phys. B **103**, 809 (2011).
5. S. P. David, V. Jambunathan, A. Lucianetti, and T. Mocek, High Power Laser Sci. Eng. **6**, 10 (2018).
6. J. Liu, L. Li, X. Shi, R. Chen, J. Wang, and W. Chen, Chin. Opt. Lett. **16**, 121402 (2018).
7. H. Yang, J. Meng, X. Ma, and W. Chen, Chin. Opt. Lett. **12**, 121406 (2014).
8. Y. G. Kim, J. H. Lee, J. Lee, Y. H. An, J. J. Dang, J. Jo, H. Y. Lee, K. J. Chung, Y. S. Hwang, and Y. S. Na, Fusion Eng. Des. **96**, 882 (2015).
9. J. Qiu, X. Tang, Z. Fan, H. Wang, and H. Liu, Appl. Opt. **55**, 5630 (2016).
10. W. Koechner, *Solid-State Laser Engineering* (Springer-Verlag, 1999).
11. X. D. Xu, X. D. Wang, J. Q. Meng, Y. Cheng, D. Z. Li, S. S. Cheng, F. Wu, Z. W. Zhao, and J. Xu, Laser Phys. Lett. **6**, 678 (2009).
12. D. C. Brown, C. D. McMillen, C. Moore, K. W. Joseph, and V. Envid, J. Lumin. **148**, 26 (2014).
13. H. Aman and A. Aman, J. Russ. Laser Res. **34**, 295 (2013).
14. J. Ma, T.-T. Lu, P.-X. Zhang, X.-L. Zhu, Y. Hang, and W.-B. Chen, Opt. Quantum Electron. **47**, 3213 (2015).
15. Q. Liu, M. Gong, T. Liu, Z. Sui, and X. Fu, Opt. Lett. **41**, 5322 (2016).
16. Z. Kang, Z. Fan, Y. Huang, H. Zhang, W. Ge, M. Li, X. Yan, and G. Zhang, Opt. Express **26**, 6560 (2018).